Pergamon

European Journal of Cancer Vol. 31A, No. 5, pp. 766–770, 1995

0959-8049/95 $9.50+0.00

0959-8049(94)00514-1

Influence of Molecular Weight on Passive Tumour Accumulation of a Soluble Macromolecular Drug Carrier

L.W. Seymour, Y. Miyamoto, H. Maeda, M. Brereton, J. Strohalm, K. Ulbrich and R. Duncan

The molecular weight-dependence of tumour capture of *N*-(2-hydroxypropyl)methacrylamide (HPMA) copolymers (fractions of mw 22 000–778 000) was studied *in vivo* using subcutaneous (s.c.) Sarcoma 180 or B16F10 melanoma models. At 10 min, all fractions were already detectable in the tumour (1.5–3% of dose administered per gram) and those of molecular weight greater than the renal threshold showed progressive tumour accumulation up to 20% of dose administered per gram after 72 h in the Sarcoma 180 model. Tumour-selective uptake was confirmed for all copolymer fractions in both tumour models and in the sarcoma 180 model, the ratio (accumulation index, AI) of the AUC in tumour to AUC in skeletal muscle (a typical normal tissue) increasing from six to 12 with increasing copolymer molecular weight. The tumour/blood AI was greater (1–3) in the Sarcoma 180 model than the B16F10 melanoma model (0.4–1.0).

Key words: polymer conjugates, targeting, *N*-(2-hydroxypropyl)methacrylamide copolymers, vascular permeability

Eur J Cancer, Vol. 31A, No. 5, pp. 766–770, 1995

INTRODUCTION

SOLUBLE MACROMOLECULES such as albumin [1], conjugates of neocarzinostatin and styrene maleic anhydride (SMANCS) [2–4], and polymeric drug carriers, such as copolymers of *N*-(2-hydroxypropyl)methacrylamide (HPMA) [5–6], have the ability to accumulate preferentially in solid tumours (reviewed in [7]). This phenomenon was termed enhanced permeability and retention (EPR effect) by Matsumura and Maeda [8], and it results from the increased permeability of tumour vascular endothelium towards circulating macromolecules, combined with limited lymphatic drainage in the tumour interstitium [4, 9]. The EPR effect is thought to contribute to the impressive anti-tumour activity of SMANCS in the treatment of primary hepatoma and other tumours [10–13].

Matsumura and Maeda [8] have already shown that following intravenous (i.v.) administration of a series of proteins (molecular weights in the range Mr 12 000 to 160 000) to mice bearing subcutaneous (s.c.) Sarcoma 180 tumours, larger proteins take longer to reach a tumour:blood ratio of 5, probably indicating less efficient leakage across the tumour endothelial barrier with increasing substrate size. Very recently, Li and associates [14] confirmed this effect following i.v. administration of SMANCS and [^{51}Cr]bovine serum albumin to rats bearing Walker sarcoma. Although proteins provide a logical tool to study the EPR effect, they afford the disadvantage that each protein presents a unique conformation and charge, and can be subject to denaturation or degradation, making it impossible to study systematically only the effect of substrate size.

Anthracyclines covalently bound to HPMA copolymers show improved anti-tumour activity in many solid tumour models (reviewed in [15]), and the EPR effect contributes to their mechanism of action. Selective accumulation of HPMA copolymer daunomycin (Dnm) was first demonstrated using a s.c. Walker sarcoma model [5], and HPMA copolymer doxorubicin (Dox) also displayed the EPR effect in s.c. B16 melanoma [6]. The purpose of this study was to investigate systematically the molecular weight dependence of EPR in two s.c. tumour models; sarcoma 180 and B16 melanoma, using a series of HPMA copolymer fractions (mw in the range 22 000–778 000) of very narrow polydispersity, each including methacryloyltyrosinamide (approximately 1 mol%) to permit radioiodination (Table 1). Polymers were administered i.v., and their plasma clearance and deposition in tumour measured. In certain studies, renal clearance, deposition in muscle adjacent to the tumour, and accumulation in liver, spleen and skin were also investigated. For comparative purposes, mouse serum albumin (MSA) and mouse immunoglobulin (IgG) were also used as substrates.

MATERIALS AND METHODS

Materials

HPMA copolymer fractions (Table 1) were prepared as described previously [16]. Briefly, monomers of HPMA [17] and

Correspondence to: Professor R. Duncan at the School of Pharmacy, University of London, Brunswick Square, London WC1N 1AX, U.K.
L.W. Seymour and R. Duncan were at the Cancer Research Campaign's Polymer-Controlled Drug Delivery Group, Department of Biological Sciences, Keele University, Staffordshire ST5 5BG, U.K.; Y. Miyamoto and H. Maeda are at the Department of Microbiology, Kumamoto University School of Medicine, Kumamoto 860, Japan; and J. Strohalm and K. Ulbrich are at the Institute of Macromolecular Chemistry, Czech Republic Academy of Sciences, Prague 6, Czech Republic; and M. Brereton was at the Birmingham Institute for Cancer Studies, University of Birmingham, Edgbaston, Birmingham B15 2TT, U.K.
Revised 18 Aug. 1994; accepted 5 Sep. 1994.

Table 1. Characteristics of HPMA copolymer fractions

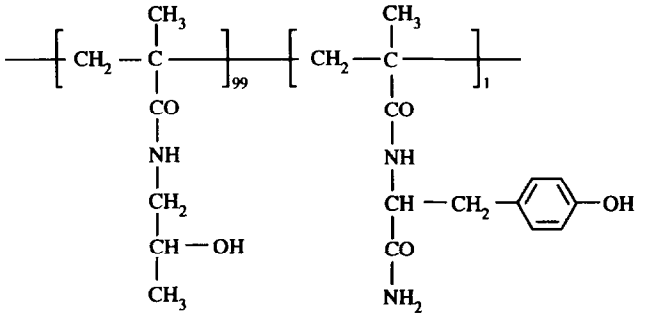

Substrate	Molecular weight average (mw)	mw/mn*
1	778 000	1.2
2	556 000	1.2
3	297 000	1.2
4	148 000	1.2
5	78 000	1.2
6	40 000	1.2
7	22 000	1.2

* Calculated by gel permeation chromatography using polyHPMA as reference standards.

methacryloyltyrosinamide (MA-TyrNH_2) [18] were prepared and then polymerised by radical precipitation polymerisation [19, 20]. The resultant copolymer preparation was fractionated using Sepharose 4B/6B (1/1 mixture, column length 85 cm, internal diameter 16 mm, eluent Tris–HCl buffer 0.05 M containing 0.5 M NaCl, pH 8.0) to give seven fractions. Each fraction was dialysed against water, using an ultrafiltration cell and an Amicon membrane UM05 (0.3 MPa), and lyophilised using a Leybold-Heraeus GT-2 apparatus. The extent of incorporation of the MA-TyrNH_2 was assessed by UV spectroscopy, and was approximately 1 mol% in each fraction.

Mouse serum albumin (MSA) and non-specific murine IgG (IgG) were purchased from Sigma (Poole, Dorset, U.K.).

Radioiodination of substrates

HPMA copolymer fractions and the proteins were radiolabelled using the Chloramine T method, either with the reagent free in solution or immobilised on Iodobeads (Pierce Chemicals, Rockford, U.S.A.). The methods have been described previously [18, 21], and following iodination, free [^{125}I]iodide was removed by Sephadex G-25 column chromatography. The specific radioactivity of all substrates was approximately 80 μCi/mg. Immediately prior to administration, all radioiodinated substrates were again subjected to Sephadex G-25 column chromatography to remove free [^{125}I]iodide, and they contained less than 1% free iodide at the time of use.

In vivo *tumour models*

Sarcoma 180 model: male ddY, 6-week-old mice (35–40 g, from the colony of the Kumamoto University School of Medicine, Japan) were injected s.c. with 10^6 Sarcoma 180 cells isolated from ascitic fluid of tumour-bearing mice. The tumours were palpable by day 5, and distribution studies were undertaken on day 9 when tumour diameters were 7–10 mm.

B16F10 melanoma model: male C57 mice, 22 g, aged 6–8 weeks (from Bantin and Kingman Ltd, U.K.) were injected s.c. with 10^5 B16F10 melanoma cells. Tumours were palpable after 11–12 days and distribution studies were routinely carried out on day 13 when tumour diameters were 9–10 mm.

Body distribution and tumour accumulation studies

Copolymer fractions 1–7 were administered to mice via the lateral tail vein (10 μg substrate in 0.1 ml phosphate-buffered saline). At various times (10 min, 30 min, 1, 3, 6, 12, 24, 48 and 72 h) mice were killed, and in all experiments blood samples were taken (by cardiac puncture in ddY and from the tail vein in C57 mice), and the tumours isolated and weighed. Urine and faeces were collected throughout the course of the experiments, and in the case of the Sarcoma 180 model, additional tissue samples were taken and weighed including muscle, liver, spleen and skin. Tissue samples were homogenised and all samples were analysed for radioactivity. In the case of the B16F10 model, the whole carcass was dissolved in NaOH (10 M, 85°C, 3 h), and the radioactivity was measured to enable estimation of total recovery of dose administered. The total blood radioactivity was calculated on the basis of a blood volume of 8.64 ml/100 g mouse body weight [22].

Data describing the distribution of radiolabelled substrates in different organs and tissues are expressed as the percentage of the administered dose of radioactivity recovered (per g) in each organ or tissue. Distribution parameters were further defined by measuring the area under the concentration–time curve (AUC) for specific tissues or blood from 0 to 72 h, and subsequently calculating accumulation indices (AI), defined as the ratio of AUC in one tissue or tumour compartment divided by the equivalent AUC for another.

RESULTS

HPMA copolymer fractions showed profiles of blood clearance that were strongly dependent on molecular size (Figure 1). The lowest molecular weight fraction 7 (mw 22 000) was rapidly cleared from the bloodstream with a $t_{\frac{1}{2}}$ (time taken to reach 50% of the initial plasma value) of less than 10 min in both C57 and ddY mice. It should be noted that ddY mice were approximately twice the weight of C57 mice, and thus their larger blood volume gave rise to the differences in blood levels of radioactivity when expressed in terms of % of dose administered/g. Blood clearance of radioactivity in ddY mice showed good correlation with urinary excretion of radiolabelled polymer, for example, following administration of fraction 6 (mw 40 000) approximately 60% of dose administered was detected in the urine after 24 h (results not shown). Fraction 6, being near to the estimated threshold for renal excretion of HPMA copolymers (mw ~ 45 000, [16]), was cleared more slowly than fraction 7, having a $t_{\frac{1}{2}}$ of 30 min in ddY mice. The higher molecular weight HPMA copolymer fractions were unable to pass through the kidney glomerulus (24 h urine levels <15% of dose) and had long circulation times, with $t_{\frac{1}{2}}$ values of 20–24 h in both strains of mouse.

Following i.v. injection to C57 mice, the protein substrates displayed a pattern of clearance intermediate between that of the large and small copolymer fractions and consistent with time-dependent substrate degradation (Figure 1a). IgG had an initial $t_{\frac{1}{2}}$ of 10.8 h, with 21.6% of the dose remaining in the circulation after 72 h. MSA was cleared faster, the initial $t_{\frac{1}{2}}$ being 4.1 h, with only 6.8% of the dose remaining in circulation after 72 h. These results are very similar to those reported following i.v. administration of [^{51}Cr]IgG and MSA to ddY mice [8].

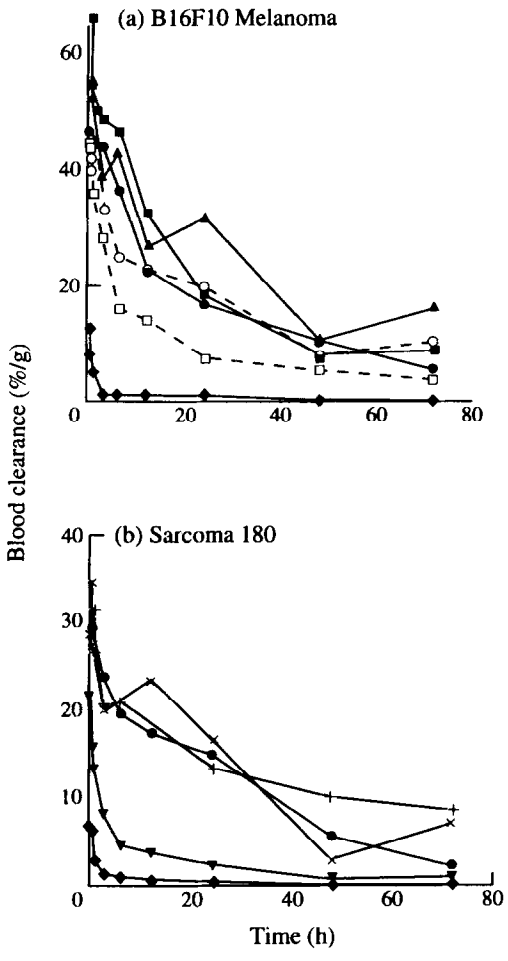

Figure 1. Blood clearance of ^{125}I-labelled macromolecular substrates (see Table 1 for details) following i.v. administration to (a) C57 mice bearing established s.c. B16F10 melanoma or (b) ddY mice bearing Sarcoma 180. Duplicate blood samples were taken at the time of sacrifice, and each point represents one individual. Clearance of HPMA copolymers is shown (a): substrates 1 (■—■), 3 (▲—▲), 5 (●—●), 7 (◆—◆), and proteins IgG (○—○) and albumin (□—□), (b): substrates 2 (×—×), 4 (+—+), 5 (●—●), 6 (▼—▼), 7 (◆—◆).

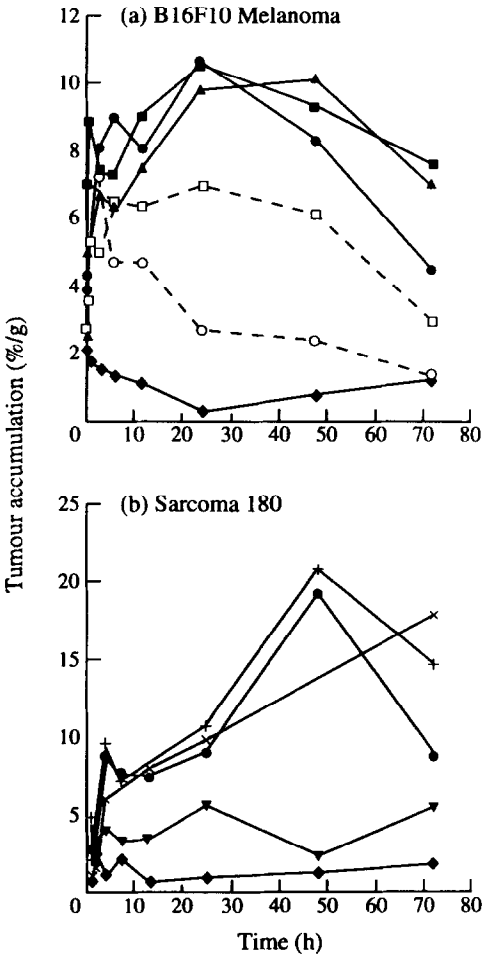

Figure 2. Tumour accumulation of ^{125}I-labelled macromolecular substrates (see Table 1 for details) following i.v. administration to (a) C57 mice bearing s.c. B16F10 melanoma, or (b) ddY mice bearing established s.c. Sarcoma 180. Blood samples were taken at the time of sacrifice, and each point represents one individual. Tumour accumulation of HPMA copolymers is shown (a) substrates 1 (■—■), 3 (▲—▲), 5 (●—●), 7 (◆—◆), and proteins IgG (○—○) and albumin (□—□), (b): substrates 2 (×—×), 4 (+—+), 5 (●—●), 6 (▼—▼), 7 (◆—◆).

The initial tumour levels of all HPMA copolymer fractions were virtually independent of substrate size in both tumour models (Figure 2). In the Sarcoma 180 model, all fractions showed a 10-min level of approximately 1.5%/g whereas in B16F10 melanoma the average value was approximately 3%/g. This difference could be attributed to the initial differences in blood volume in the two strains of mouse. With time, the smaller copolymer fractions, 7 and 6 (mw 22 000 and 40 000), did not show progresive accumulation in tumour tissue, whereas the larger fractions, 1–5 (mw ≥ 78 000), showed progressive accumulation over 24 h. In the B16F10 melanoma model, the maximum value attained by the larger copolymer fractions was approximately 10%/g, after 24 h. This value apparently fell after 72 h, probably due to the rapid increase in tumour size. In the Sarcoma 180 model, levels of 10%/g were also achieved after 24 h, although some animals did show accumulation as high as 20%/g after 48–72 h. Relatively low levels of radioactivity were found in liver, spleen, muscle and skin following i.v. administration of ^{125}I-labelled HPMA copolymers to ddY mice (Figure 3), without any evidence for time-dependent accumulation, except in skin where substrates of mw > 78 000 did progressively accumulate 12–48 h postinjection (up to 7%/g).

Expression of radioactivity levels as AUC (between 0–72 h) (Figure 4a) showed obvious differences between the two strains of mice/tumour models. Whereas the Sarcoma 180 model displayed a tumour/blood AI which was greater than 1 for all molecular weight fractions, the B16F10 model displayed values which were consistently 3-fold lower. In the Sarcoma 180 model sampling of muscle tissue permitted calculation of the tumour/muscle AI, and this index increased from six to 12 with increasing polymer size (Figure 4b). Protein substrates showed more rapid loss from the bloodstream, and less efficient accumulation in B16 melanoma than the higher molecular weight polymers, the tumour/blood AI in C57 mice for both MSA and IgG being 0.33 and 0.37, respectively. These values are comparable with those seen for polymers of equivalent size. Quantitative comparison is difficult, however, as these protein substrates suffer proteolytic degradation during the course of the experiment, whereas the polymer substrates do not degrade.

DISCUSSION

Polymer conjugates constitute a new class of anti-tumour agents, and recently two polymer–protein conjugates, SMANCS

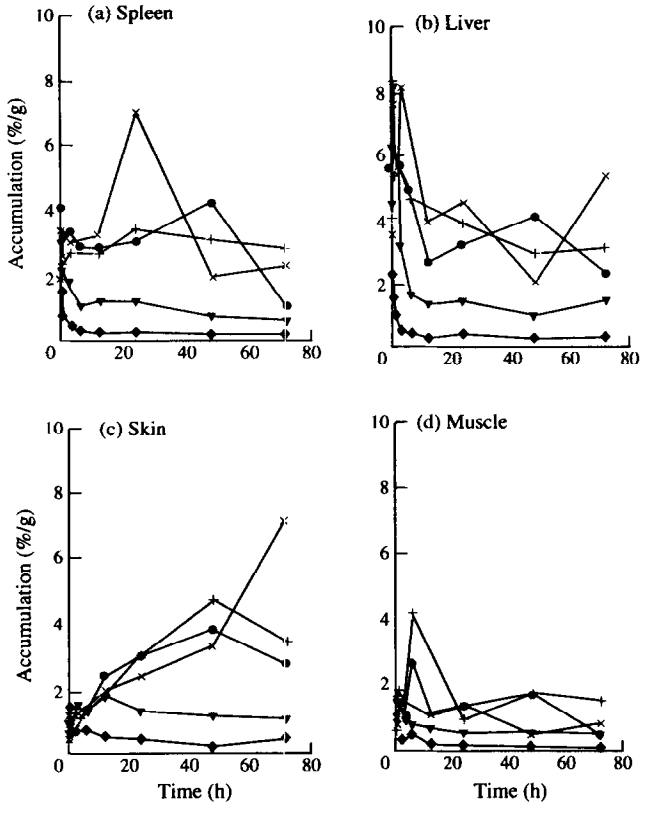

Figure 3. General tissue distribution of ^{125}I-labelled HPMA copolymers following i.v. administration to ddY mice bearing established s.c. Sarcoma 180. Radioactivity detected in the tissues following administration of HPMA copolymers 2 (×—×), 4 (+—+), 5 (●—●), 6 (▼—▼), 7 (◆—◆) is shown.

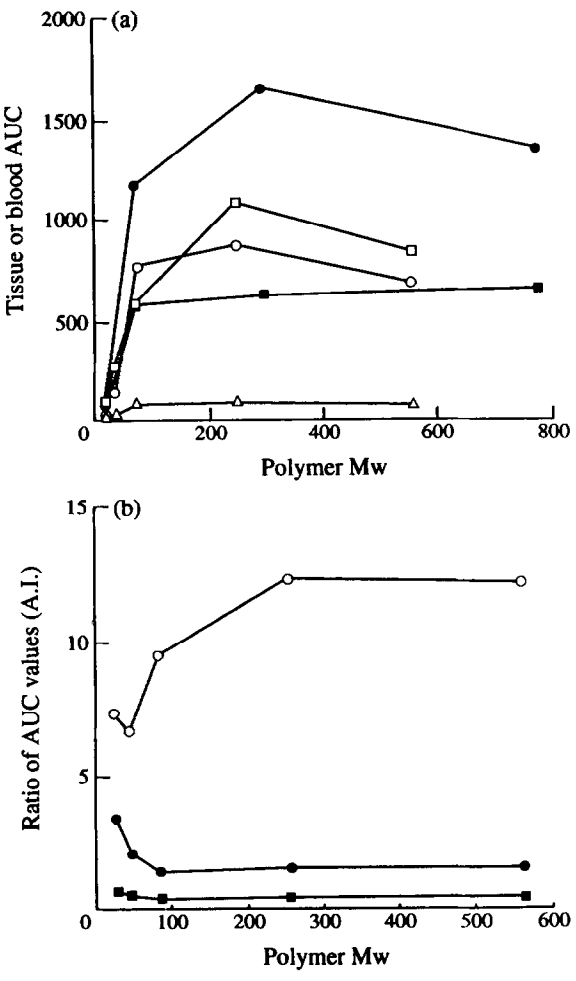

Figure 4. Distribution parameters measured for ^{125}I-labelled HPMA copolymers following i.v. administration to ddY mice bearing established s.c. Sarcoma 180 or C57 mice bearing B16F10 melanoma. (a) shows the AUC (calculated 0–72 h after administration) for tumour radioactivity in the B16F10 model (■—■) and the sarcoma 180 model (□—□), the blood AUC for C57 (●—●) and ddY (○—○) mice, and also the muscle AUC for ddY mice (△—△). (b) shows the relationship between AI and polymer molecular weight for tumour/blood (●—●), muscle/blood (■—■) and tumour/muscle (○—○) calculated from data obtained in the sarcoma 180 model.

[10–13] and polyethyleneglycol-L-asparaginase [23], were approved for clinical use for treatment of primary hepatoma (intrahepatic arterial administration in Lipiodol) and acute lymphocytic leukaemia (patients hypersensitive to L-asparaginase), respectively. As we have begun to realise the general importance of the EPR effect in localising macromolecules within solid tumours, it has become obvious that there is a need to synthesise polymer–drug conjugates with polymer characteristics selected to optimise their passive tumour targeting by EPR. Ability to tailor favourable toxicity- and efficacy-related chemical characteristics of polymer conjugates bearing conventional chemotherapeutic agents will ultimately govern their therapeutic potential. Here we established that HPMA copolymers show a high degree of tumour localisation in Sarcoma 180 and B16F10 mouse tumour models, thus adding to our earlier observation which showed higher localisation of HPMA copolymer daunomycin in Walker sarcoma [5] than as seen for free drug.

HPMA copolymers are neutral, loosely coiled macromolecules which do not have natural affinity for the plasma membrane, and thus are captured slowly by cells via the mechanism of fluid-phase pinocytosis. Following i.v. administration, smaller HPMA copolymer molecules (<mw 40 000) are subject to rapid renal clearance, but owing to their size, higher molecular weight polymers find it impossible to escape via the kidney and persist in the circulation for long periods (Figure 1). Blood concentration of HPMA copolymer with time proved the most important determinant of subsequent polymer levels measured in both tumour (Figure 2) and normal tissues (Figure 3). Generally, HPMA copolymer levels in normal tissues were very low, with the exception of liver, which displayed an elevated early concentration that declined with time, probably reflecting the high concentration of polymer initially entrapped in the liver intravascular space. The only normal tissue which showed time-dependent accumulation of high molecular weight polymers (mw 560 000 > 150 000 > 80 000) was the skin, and this phenomenon has been reported previously [24]. Clinical application of macromolecular drug carriers demands the choice of a molecular weight that will not accumulate in the skin, thus avoiding the risk of skin-related toxicity. The HPMA copolymers of molecular weight sufficiently high to escape glomerular filtration exhibited time-dependent tumour accumulation and achieved maximum tumour levels of 10–20%/g tumour (Figure 2). These values are greater than many reported for localisation of proteins and anti-tumour antibodies in mouse tumours; for example, 3.7%/g in M21 human melanoma xenograft [25] and 11.8%/g and 6 (8%/g in human small cell lung cancer xenografts [26] and [27], respectively), and similar to those reported previously for polymers, such as dextrans [28] and SMANCS [29]. As the

highest tumour/blood AI values were observed for the smallest polymer substrates, it can be concluded that low molecular weight HPMA copolymers have significant advantage in context of tumour imaging. In context of drug targeting, higher molecular weight polymer-drug conjugates would localise more drug in the tumour. However, it remains to be seen whether this would result in an improved therapeutic index due to the lower tumour/blood AI of these polymers and their lower rate of whole body excretion. It seems probable that higher molecular weight polymer–drug conjugates would be more toxic, as well as potentially more efficacious.

It was noteworthy that the tumour/blood AI values seen for Sarcoma 180 were on average 3-fold higher than those measured for B16F10 melanoma (Figure 4a). This could be due to differences in the degree of tumour vascularisation in the two tumour types; increased permeability of the vasculature in the sarcoma 180 model, giving an apparently higher tumour AUC; or may reflect differences in the rate of renal clearance/extravasation and warrants further investigation. The tumour/muscle AI measured in Sarcoma 180 displayed a value greater than unity for all molecular sizes (Figure 4b), confirming that polymers which persist in the bloodstream gain easier entry into tumour rather than muscle (as a representative normal tissue). As the tumour/muscle AI rises with increasing polymer molecular weight, a differential permeability between tumour endothelium and that serving normal muscle is suggested. The efficacy of macromolecular drug carriers is influenced not only by tumour levels, but also intra-tumoral distribution. Preliminary studies using fluorescence-labelled HPMA copolymers in conjunction with the B16F10 tumour model have shown that HPMA copolymers of molecular weights in the range used here do undergo extravasation (10 min), predominantly in the fibrous vascularised stromal regions [6].

1. Sinn H, Shrenk HH, Freidrich EA, Schilling U, Maier-Borst W. Design of compounds having an increased tumour uptake, using serum albumin as carrier. Part 1. *Nucl Med Biol* 1990, **17**, 819–827.
2. Maeda H, Takeshita J, Kanamaru R. A lipophilic derivative of neocarzinostatin: a polymer conjugation of an antitumour protein antibiotic. *Int J Peptide Protein Res* 1979, **14**, 81–87.
3. Maeda H, Matsumoto T, Konno T, Iwai K, Ueda M. Tailor-making of protein drugs by polymer conjugation for tumor targeting: a brief review on smancs. *J Protein Chem* 1984, **3**, 181–193.
4. Maeda H. The tumour blood vessel as an ideal site for macromolecular anticancer agents. *J Controlled Rel* 1992, **19**, 315–324.
5. Cassidy J, Duncan R, Morrison GJ, *et al.* Activity of *N*-(2-hydroxypropyl)methacrylamide copolymers containing daunomycin against a rat tumour model. *Biochem Pharmacol* 1989, **38**, 857–879.
6. Seymour LW, Ulbrich K, Brereton M, *et al.* Tumouritropism and anticancer efficacy of polymer-based doxorubicin prodrugs in the treatment of subcutaneous murine B16F10 melanoma. *Br J Cancer* 1994, in press.
7. Seymour LW. Passive tumour targeting of soluble macromolecules and drug conjugates. *CRC Crit Rev Therapeut Drug Carrier Syst* 1992, **9**, 135–187.
8. Matsumura Y, Maeda H. A new concept for macromolecular therapeutics in cancer therapy: mechanism of tumoritropic accumulation of proteins and the antitumor agent SMANCS. *Cancer Res* 1986, **46**, 6387–6392.
9. Maeda H, Seymour LW, Miyamoto Y. Conjugates of anticancer agents and polymers: advantages of macromolecular therapeutics *in vivo*. *Bioconjugate Chem* 1992, **3**, 351–362.
10. Konno T, Maeda H, Mochinga M, Tashiro S, Uchida M, Yokoyama I. Effect of arterial administration of high molecular weight anticancer agent SMANCS with lipid lymphographic agent on hepatoma: a preliminary report. *Eur J Cancer Clin Oncol* 1983, **19**, 1053–1065.
11. Konno T. Targeting chemotherapy for hepatoma: arterial administration of anticancer drugs dissolved in Lipiodol. *Eur J Cancer* 1992, **28A**, 403–409.
12. Kimoto A, Konno T, Kawaguchi T, Miyauchi Y, Maeda H. Antitumour effects of SMANCS on rat mammary tumor induced by 7,12-dimethylbenz[a]anthracene. *Cancer Res* 1992, **52**, 1013–1017.
13. Maeda H. SMANCS and polymer-conjugated macromolecular drugs: advantages in cancer chemotherapy. *Adv Drug Deliv Rev* 1991, **6**, 181–202.
14. Li CJ, Miyamoto Y, Kojima Y, Maeda H. Augmentation of tumour delivery of macromolecular drugs with reduced bone marrow delivery by elevating blood pressure. *Br J Cancer* 1993, **67**, 975–890.
15. Duncan R. Drug-polymer conjugates: potential for improved chemotherapy. *Anti-Cancer Drugs* 1992, **3**, 175–210.
16. Seymour LW, Duncan R, Strohalm J, Kopecek J. Effect of molecular weight of *N*-(2-hydroxypropyl)methacrylamide copolymers on body distribution and rate of excretion after subcutaneous, intraperitoneal and intravenous administration to rats. *J Biomed Mater Res* 1987, **21**, 1341–1358.
17. Strohalm J, Kopecek J. Poly[*N*-(2-hydroxypropyl)methacrylamide]. IV. Heterogeneous polymerisation. *Angew Makromol Chem* 1978, **70**, 109–115.
18. Duncan R, Kopecek J, Rejmanova P, Lloyd JB. Targeting of *N*-(2-hydroxypropyl)methacrylamide copolymers to liver by incorporation of galactose residues. *Biochim Biophys Acta* 1983, **755**, 518–521.
19. Kopecek J. Reactive copolymers of *N*-(2-hydroxypropyl)methacrylamide with *N*-methacryloylated derivatives of L-leucine and L-phenylalanine. I. Preparation, characterisation and reaction with diamines. *Makromol Chem* 1977, **178**, 2169–2183.
20. Kopecek J, Rejmanova P. Reactive copolymers of *N*-(2-hydroxypropyl)methacrylamide with *N*-methacryloylated derivatives of L-leucine and L-phenylalanine. II. Reaction with the polymeric amine and stability of the crosslinks towards chymotrypsin. *J Polymer Sci Polymer Symp* 1979, **66**, 209–218.
21. Seymour LW, Flanagan PA, Al-Shamkhani A, *et al.* Synthetic polymers conjugated to monoclonal antibodies: vehicles for tumour-targeted drug delivery. *Selective Cancer Therapeut* 1991, **7**, 59–73.
22. Seymour LW, Ulbrich K, Wedge SR, Hume IC, Strohalm J, Duncan R. *N*-(2-Hydroxypropyl)methacrylamide copolymers targeted to the hepatocyte galactose-receptor: pharmacokinetics in DBA2 mice. *Br J Cancer* 1991, **63**, 859–866.
23. Nucci ML, Shorr R, Abuchowski A. The therapeutic values of poly(ethylene glycol)-modified proteins. *Adv Drug Delivery Rev* 1991, **6**, 133–151.
24. Goddard P, Williamson I, Brown J, Hutchinson LE, Nicholls J, Petrak K. Soluble polymeric carriers for drug delivery-part 4: tissue autoradiography and whole body distribution of *N*-(2-hydroxypropyl)methacrylamide copolymers following intravenous administration. *J Bioact Compat Polymers* 1991, **6**, 4–12.
25. Yang HM, Reisfeld RA. Doxorubicin conjugated with a monoclonal antibody directed to a human melanoma-associated proteoglycan suppresses the growth of established tumour xenografts in nude mice. *Proc Natl Acad Sci USA* 1988, **85**, 1189–1193.
26. Boerman OC, Mijnheere EP, Broers JL, Vooijs GP, Ramaekers FC. Biodistribution of a monoclonal antibody (RNL-1) against the neural cell adhesion molecule (NCAM) in athymic mice bearing human small-cell lung-cancer xenografts. *Int J Cancer* 1991, **48**, 457–462.
27. Mijnheere EP, Boerman OC, Broers JL, Klein-rot M, Vooijs GP, Ramaekers FC. Immunotargeting of human small cell lung cancer xenografts in athymic mice using a monoclonal antibody (RNL-1) against a neuroendocrine-related antigen. *Br J Cancer* 1991, **14** (suppl.), 78–81.
28. Takakura Y, Fujita T, Hashida M, Sezaki H. Disposition characteristics of macromolecules in tumour-bearing mice. *Pharm Res* 1990, **7**, 339–346.
29. Maeda H, Matsumura Y. Tumouritropic and lymphotropic principles of macromolecular drugs. *CRC Critical Rev Therap Drug Carrier Syst* 1989, **6**, 193–210.

Acknowledgements—This work was supported by the Cancer Research Campaign, Medical Research Council, and by a grant for Cancer Research from the Ministry of Education, Science and Culture, Japan. The international collaborations were sponsored by the Royal Society of London, Academy of Sciences and the Japanese Society for the Promotion of Science.